Journal Pre-proof

Robust State/Output Feedback Linearization of Direct Drive Robot Manipulators: A Controllability and Observability Analysis

Adolfo Perrusquía

PII: S0947-3580(21)00142-4
DOI: https://doi.org/10.1016/j.ejcon.2021.12.007
Reference: EJCON 612

To appear in: *European Journal of Control*

Received date: 22 August 2021
Revised date: 27 December 2021
Accepted date: 27 December 2021

Please cite this article as: Adolfo Perrusquía, Robust State/Output Feedback Linearization of Direct Drive Robot Manipulators: A Controllability and Observability Analysis, *European Journal of Control* (2022), doi: https://doi.org/10.1016/j.ejcon.2021.12.007

European Journal of Control, Volume 64, March 2022, Article number 100612
DOI:10.1016/j.ejcon.2021.12.007

Robust State/Output Feedback Linearization of Direct Drive Robot Manipulators: A Controllability and Observability Analysis

Adolfo Perrusquía

School of Aerospace, Transport and Manufacturing, Cranfield University, MK43 0AL, UK

Abstract

In this research, a robust feedback linearization technique is analysed for robot manipulators control. A complete first-order Taylor series expansion is used to linearize the robot dynamics which takes into account initial conditions and the Taylor-series remainder. A modified PD control law with Taylor-series compensation is used to guarantee robust reference tracking. Whilst classic feedback linearization controllers guarantee asymptotic convergence to zero, the proposed approach shows that, for real applications, if the linearized robot dynamics is stable then the nonlinear robot states are also stable and remain bounded. This premise is assessed via Lyapunov stability theory under a controllability and observability analysis; and hence, exponential convergence to a bounded set is concluded. Experiments are carried out using a 1-degree of freedom robot and a 4-degree of freedom exoskeleton robot to validate the proposed approach.

Keywords: Robust feedback linearization, Robot Manipulators, Exponential convergence, Controllability, Observability, Lyapunov and Riccati equations.

1. Introduction

Feedback linearization is a popular technique for real-time applications and industrial prototypes [1, 2]. It gives an interesting tool for nonlinear systems control based on its linearized approximation for small deviations of its states. The linearization procedure needs that the nonlinear system is written in the standard form [3, 4],

$$\dot{x} = f(x) + g(x)u, \tag{1}$$

where x are the states, u the control inputs and $f(x)$ and $g(x)$ are the nonlinear dynamics of the system. If the system is written as in (1), then the linearization procedure can be done. However, there a class of nonlinear systems which are the exception of this rule: robot manipulators [5].

Robot manipulators [6] are a class of nonlinear systems which seems to have no problem writing its dynamics as in (1) [7]. This is true, however when the linearization procedure is applied, the final linear model could be an oversimplified model due to the inertia matrix of the robot [8]. In other words, the presence of the inertia matrix in $f(x)$ and $g(x)$ can make zero some relevant terms when the linearization technique is applied at the desired operating point.

Typically, direct drive robot manipulators (which are the main concern of this paper) are controlled by linear or nonlinear controllers whose gains are tuned manually until an acceptable response is obtained, e.g., PID control, sliding mode control (SMC) [9], and fuzzy control [10]. In the case of PID control, there exists some rules to set its gains in accordance to the lower and upper bounds of the robot matrices [11]. However, it is not possible to establish a desired performance as in the linear case and hence, a manual tuning procedure is required. It is mandatory, to compensate the nonlinear terms of the robot manipulator in order to establish a desired performance [12].

There are some investigations of robot manipulators linearization. The classical approach is known as computed torque controller [5] which assumes complete knowledge of the robot dynamics such that the nonlinear terms are compensated and establish a desired performance given by an inner controller which is typically a proportional-derivative (PD) controller. However, two main drawbacks has this controller: (i) in most cases, only an approximate model of the nonlinear dynamics can be constructed and hence, modeling error is raised, (ii) the computational complexity of this controller is high [13] and can cause delays in the real-time implementation due to hardware and software limitations.

One of the easiest method for robot manipulators' linearization is to consider that the manipulator is endowed with a gearbox with high gear ratio (typical values are 200-500) such that the nonlinear terms are practically neglected which yields in a linear system with an approximate constant disturbance [6]. Nevertheless, this method cannot be used for direct-drive manipulators.

For direct-drive robots linearization, some methods neglects the Coriolis and gravitational torques vector [8]. However, this method yields a double integrator system [1] which is an oversimplified model of the robot dynamics. Other techniques takes into account the gravitational torques [14] and the Coriolis matrix [15] with satisfactory results. Nevertheless, some information can be lost at the linearization point because the above methods do not consider adequately the Taylor series expansion.

The final linear model obtained from the linearization procedure is used to compute a feedback controller [16] which can guarantee asymptotic stability [17, 18] of the linear dynamics and uniform stability [19] of the nonlinear robot dynamics. For this reason, this technique is known as feedback linearization. Most of industrial applications assume that if the linear model is asymptotic stable, then the states of the nonlinear model are uniformly stable and therefore, they should converge to zero [19]. However, in most cases this is false because modelling uncertainties hinder accurate realization of the task and hence, the states do not converge to zero.

One main issue of feedback linearization is concerned with robust performance and stability of the closed-loop system [20]. Robust feedback linearization is nowadays an interesting control issue for real-time and industrial applications [21, 22] such as power systems [23, 24], fuel-engine [25] and nonlinear systems [19, 26, 27]; which aims to ensure robust performance against model uncertainties with good precision results [28, 29]. Robust feedback linearization is directly related to the controller design, that is, if the linearized model is poor, then the control gains will be also poor and hence the controller will lacks of robustness.

So, in this work a robust feedback linearization controller for direct drive robot manipulators is proposed to solve the following problems:

1. Computed torque control has high computational complexity which can cause time-delays and instability of the closed-loop system.
2. It is not possible to define a desired performance in linear and nonlinear controllers for direct-drive manipulators without first applying a linearization procedure.
3. Standard Taylor-series linearization procedure of direct-drive robots can give as output an oversimplified model which cannot guarantee robust performances.
4. Correct the feedback linearization assumption, that is, if the linear model is stable, then the states of the nonlinear dynamics are asymptotic stable and converges to zero.

This paper assesses the aforementioned problems by providing the following solutions and contributions:

- A complete Taylor-series linearization procedure for direct-drive robot manipulators which takes into account the robot initial conditions and the Taylor series remainder to avoid oversimplified models and improve the control design.

- A simple robust feedback-linearization controller with Taylor-series compensation which reduces the transient time, tracking error, and the computational complexity is considerably reduced.

- Two different theorems that prove exponential stability of the linearized system dynamics to a bounded zone using a controllability and observability analysis. This is a stronger result than traditional results which only shows asymptotic stability and uniform stability [19].

Throughout this paper, $\mathbb{N}$, $\mathbb{R}$, $\mathbb{R}^n$, $\mathbb{R}^{n\times m}$ denote the spaces of natural numbers, real n-vectors, and real $n \times m$-matrices, respectively; $\lambda(A)$ denotes the eigenvalues of matrix A; $\lambda_{\min}(A)$ and $\lambda_{\max}(A)$ denotes the minimum and maximum eigenvalues of matrix A, respectively; the norms $\|A\| = \sqrt{\lambda_{\max}(A^\top A)}$ and

$\|x\|$ stand for the induced Frobenius and vector Euclidean norms, respectively; where $x \in \mathbb{R}^n$, $A \in \mathbb{R}^{n\times n}$ and $n, m \in \mathbb{N}$.

2. Robot Dynamics and Robust Feedback Linearization

The dynamic model of a n degree of freedom (DOF) direct-drive robot manipulator is ,

$$M(q)\ddot{q} + C(q,\dot{q})\dot{q} + F\dot{q} + G(q) = u, \tag{2}$$

where $M(q) \in \mathbb{R}^{n\times n}$ is a positive definite inertia matrix, $C(q,\dot{q}) \in \mathbb{R}^{n\times n}$ denotes the centripetal and Coriolis forces matrix, $F \in \mathbb{R}^n$ is the friction vector, $G(q) \in \mathbb{R}^n$ is the gravitational torques vector, $u \in \mathbb{R}^n$ denotes the control torque and $q, \dot{q}, \ddot{q} \in \mathbb{R}^n$ are the joint position, velocity and acceleration vectors, respectively.

Linearization is performed with respect to an operating point $O(u_l, q_l, \dot{q}_l, \ddot{q}_l)$; where u_l is a nominal torque and $q_l, \dot{q}_l, \ddot{q}_l$ are nominal joint position, velocity and acceleration vectors. Define $q_r = q - q_l$ as the deviation between the current joint position q and the nominal value q_l. The linearization method lies in a first-order Taylor expansion as,

$$f(x) = f(x_0) + \frac{\partial f(x)}{\partial x}\Big|_{x=x_0}(x - x_0) + \varepsilon,$$

where $f(x)$ is a smooth nonlinear function, x_0 denotes an operating point and ε denotes a residual error of the Taylor expansion.

There exists several linearization methods for direct-drive robot manipulators. The most simple method neglects the Coriolis, friction and gravitational terms, that is, $C(q,\dot{q})\dot{q} = F\dot{q} = G(q) = 0$. The resulting model is a double integrator system of the form,

$$A\ddot{q}_r = u, \tag{3}$$

where $A = M(q)|_O$. The system (3) is an oversimplified model which is unstable but controllable and cannot guarantee reference tracking because the gravitational, friction and Coriolis terms should be taken into account [15]. Other linearization methods neglects the Coriolis and friction terms for small joint velocities obtaining the next linear model,

$$A\ddot{q}_r + Bq_r = u, \tag{4}$$

where $A = M(q)\big|_O$ and $B = \frac{\partial G(q)}{\partial q}\big|_O$. Model (4) has good results for control purposes since the gravity loading is a dominant component of the robot dynamics. In [8] it has been shown that the Coriolis and friction terms should be taken into account even at low joint speeds; hence the next linear model is obtained,

$$A\ddot{q}_r + D\dot{q}_r + Bq_r = u, \tag{5}$$

where $A = M(q)\big|_O$, $B = \frac{\partial (C(q,\dot{q})\dot{q}+G(q))}{\partial q}\big|_O$ and $D = \frac{\partial C(q,\dot{q})\dot{q}+F\dot{q}}{\partial \dot{q}}\Big|_O$. Model (5) has better results than (4) and has been used to obtain tuning techniques for PID controllers [15, 30]. Notice that models (3),(4) and (5) do not use adequately the Taylor series expansion since the operating point O can make zero the terms B and D. Our first contribution modifies the definitions of (5) using the first-order Taylor series expansion as,

$$A\ddot{q}_r + D\dot{q}_r + Bq_r + B_0 = u + \varepsilon_f, \tag{6}$$

with $B_0 = [G(q) + (C(q,\dot{q}) + F)\dot{q}]\Big|_O \in \mathbb{R}^n$. $\varepsilon_f \in \mathbb{R}^n$ is the remainder of the Taylor series. Notice that: (i) B_0 serves as a compensation term, especially of the gravitational torques vector, (ii) the Taylor series remainder ε_f gives a correct formulation of the linearization procedure. Classic approaches [8] do not consider ε_f which is a strong and wrong assumption for the design of robust-feedback controllers and uniform stability conclusion.

3. Control design and gains setting

A standard choice at industry and real-time applications for the feedback control torque u is a Proportional-Derivative (PD) control law [31, 32] as,

$$u = K_p e + K_d \dot{e}, \tag{7}$$

where $K_p, K_d > 0 \in \mathbb{R}^{n\times n}$ are the proportional and derivative gain matrices, $e = q_d - q_r \in \mathbb{R}^n$ defines the position error, $\dot{e} = \dot{q}_d - \dot{q}_r \in \mathbb{R}^n$ the velocity error and $q_d \in \mathbb{R}^n$ is a desired reference. Other advance controllers such as PID [21], or sliding-mode control (SMC) [29, 33, 34] can also be used. However in this paper a PD control law is used for simplicity and to avoid biased conclusions of the proposed method.

The PD control (7) is slightly modified by adding a compensation of the Taylor-series components as

$$u = K_p e + K_d \dot{e} + B_0 + Bq_d + D\dot{q}_d + A\ddot{q}_d. \tag{8}$$

The above controller is in fact a feedback linearization controller [28] in terms of Taylor-series components. The closed-loop system between (6) and (8) is,

$$\ddot{e} + A^{-1}(D + K_d)\dot{e} + A^{-1}(B + K_p)e + \eta = 0 \tag{9}$$

where $\eta = A^{-1}\varepsilon_f$. Then (9) can be expressed as a linear system with desired performance as,

$$\ddot{e} + \Lambda_1\dot{e} + \Lambda_2 e + \eta = 0, \tag{10}$$

where $\Lambda_1, \Lambda_2 > 0 \in \mathbb{R}^{n\times n}$ define a desired closed-loop performance, similarly to a pole-placement control problem.

Remark 1. *Let $\eta = 0$. Then, the desired response of the tracking error e is defined in how we choose Λ_1 and Λ_2. If the roots of the characteristic polynomial $s^2 I + s\Lambda_1 + \Lambda_2$ have negative real part then the trajectories will converge exponentially to zero. Conversely, if the roots have positive real part, then the trajectories of e will diverge. In this work, Λ_1 and Λ_2 are chosen to satisfy a perfect square trinomial and therefore, the roots have a negative real part.*

Remark 2. *Matrix A amplifies or attenuates the performance matrices Λ_1 and Λ_2. This linear transformation is directly reflected in the final control gains K_p and K_d and provides a first approximation in the possible range of values for Λ_1 and Λ_2 that we can use for the gain tuning.*

From (10), the PD gains are tuned as: $K_p = A\Lambda_2 - B$ and $K_d = A\Lambda_1 - D$. Notice that if the linearized model does not consider matrices B and D, then the control gains K_p and K_d will be larger which can cause oscillations, overdamped responses or even instability of the robot trajectories.

The state-space representation of (9) is,

$$\dot{x} = \underbrace{\begin{bmatrix} 0 & I \\ -A^{-1}(B+K_p) & -A^{-1}(D+K_d) \end{bmatrix}}_{A_K \in \mathbb{R}^{2n\times 2n}} x + \underbrace{\begin{bmatrix} 0 \\ -\eta \end{bmatrix}}_{\xi \in \mathbb{R}^{2n}} \tag{11}$$

where $x = [e^\top, \dot{e}^\top]^\top \in \mathbb{R}^{2n}$. The eigenvalues $\lambda(A_k)$ of matrix A_k have negative real part $\mathrm{Re}\lambda_i(A_k) < 0$ and verifies the model (10), that is, $\det(\lambda I - A_K) = \lambda^2 + \Lambda_1\lambda + \Lambda_2$. Since ε_f is bounded, then $\|\xi\| \leq \bar{\xi}$ is also bounded.

Remark 3. *The dynamics of the manipulator is linearized in an operating point O such that the linearized model behaves as the nonlinear dynamics valuated in the operating point. It is well known that the remainder of the Taylor formula decreases as we take more terms in the series. Moreover, high order terms are very small in comparison to the first order terms as it is stated by the Lagrange error bound [35]. Therefore, if the linear system is stabilizable by the PD control law, then the nonlinear system will be also stabilizable. Furthermore, the remainder of the Taylor formula can be modelled as the disturbance caused by the robot nonlinear dynamics which can be attenuated by the PD gains and Taylor series compensation.*

4. Stability

In this section, the stability of the closed-loop performance (11) is analyzed using two methods: controllability and observability [36] approaches. Both methods are used to obtain the compact set in which the states will converge. In other words, the main goal is to demonstrate that the trajectories of the linearized robot dynamics converges exponentially to zero only if the residual term $\xi = 0$, otherwise the trajectories will converge exponentially to a compact set centered in zero [37].

4.1. Controllability approach

For the controllability approach [38], the closed-loop dynamics (11) can be written as,

$$\begin{aligned} \dot{x} &= A_2 x + B_2 u + \xi \\ u &= -Kx, \end{aligned} \tag{12}$$

where $A_2 \in \mathbb{R}^{2n\times 2n}$, $B_2 \in \mathbb{R}^{2n\times n}$ and $K \in \mathbb{R}^{n\times 2n}$ are defined as,

$$A_2 = \begin{bmatrix} 0 & I \\ -A^{-1}B & -A^{-1}D \end{bmatrix}, \quad B_2 = \begin{bmatrix} 0 \\ A^{-1} \end{bmatrix}$$
$$K = \begin{bmatrix} K_p & K_d \end{bmatrix}.$$

The controllability matrix of (12) is,

$$\mathcal{C} = \begin{bmatrix} B_2 & A_2 B_2 & A_2^2 B_2 & \dots & A_2^{2n-1} B_2 \end{bmatrix}. \tag{13}$$

It is known that the system states of (12) are controllable if rank $\mathcal{C} = 2n$ [39, 40]. Equivalently, the controllability of system (12) implies that the matrix

$$W_c = \int_{t_0}^{t} e^{A_2(\tau - t_0)} B_2 B_2^\top e^{A_2^\top(\tau - t_0)} d\tau, \tag{14}$$

is nonsingular for any $t > 0$ [41]. The following theorem establishes the exponential convergence to zero of (12) under the PD control law (8) with $\xi = 0$.

Theorem 1. *Consider the robot dynamics (12) under the PD control law (8), the desired performance specified by (10) and set $\xi = 0$. Then there exists positive definite matrices $Q, P \in \mathbb{R}^{2n\times 2n}$ which are solution of the Lyapunov equation,*

$$A_K^\top P + P A_K = -Q. \tag{15}$$

Hence, the states of (12) converge exponentially to zero with a decay rate of $\frac{1}{2}\gamma_1$.

Proof 1. *Consider the Lyapunov function,*

$$V = x^\top P x. \tag{16}$$

The time derivative of V along the system trajectories (12) is

$$\dot{V} = x^\top (PA_K + A_K^\top P)x = -x^\top Qx. \tag{17}$$

From (17) global asymptotic stability can be concluded. To prove exponential stability let multiply (17) by the identity matrix $PP^{-1} = I$ as,

$$\dot{V} = -x^\top PP^{-1}Qx \leq -\gamma_1 V,$$

where $\gamma_1 = \lambda_{\min}(P^{-1}Q)$. The solution of the above differential equation is,

$$V(t) \leq e^{-\gamma_1 (t-t_0)} V(t_0). \tag{18}$$

So

$$\begin{aligned}\lambda_{\min}(P)\|x(t)\|^2 &\leq x^\top(t)Px(t) = V(t)\\ &\leq e^{-\gamma_1(t-t_0)}V(t_0)\\ &= e^{-\gamma_1(t-t_0)}x^\top(t_0)Px(t_0)\\ &\leq \lambda_{\max}(P)e^{-\gamma_1(t-t_0)}\|x(t_0)\|^2\end{aligned}$$

Hence, the states of (12) converges exponentially to zero and satisfies

$$\|x(t)\| \leq \sqrt{\frac{\lambda_{\max}(P)}{\lambda_{\min}(P)}} e^{-\frac{1}{2}\gamma_1(t-t_0)}\|x(t_0)\|. \tag{19}$$

This completes the proof. □

Remark 4. *If the eigenvalues of matrix A_2 have negative real part, that is, $Re\lambda_i(A_2) < 0$, then the solution P of the Lyapunov equation (15) can be expressed in terms of (14) with $Q = B_2B_2^\top$ and its called controllability Gramian.*

The next theorem establishes the uniform ultimate boundedness (UUB) [42] of the trajectories of (12) with exponential convergence to a small compact set.

Theorem 2. *Consider the robot dynamics (12) under the PD control law (8) and the desired performance specified by (10). Then there exists positive definite matrices $Q,\ P,\ R \in \mathbb{R}^{2n\times 2n}$ which satisfy the Riccati equation [43],*

$$A_K^\top P + PA_K + PRP = -Q. \tag{20}$$

Then, the states trajectories of (12) are UUB with a practical bound given by $\mu = \sqrt{\frac{1}{\lambda_{\min}(Q)\lambda_{\min}(R)}}\|\xi\|$, *and converges exponentially to a bounded set* S_ξ *of radius* μ *with a decay factor* $\frac{1}{2}\gamma_1$ *as in (19).*

Proof 2. *Consider the same Lyapunov equation (16). The time derivative of (16) along the closed loop trajectories of (12) is*

$$\dot{V} = x^\top(PA_K + A_K^\top P)x + 2x^\top P\xi$$

The following inequality is used,

$$2x^\top P\xi \le x^\top PRPx + \xi^\top R^{-1}\xi,$$

for some normalizing matrix $R \in \mathbb{R}^{2n\times 2n}$. *So,*

$$\begin{aligned}\dot{V} &\le x^\top(PA_K + A_K^\top P + PRP)x + \xi^\top R^{-1}\xi \\ &= -x^\top Qx + \xi^\top R^{-1}\xi. \end{aligned} \tag{21}$$

The time-derivative of the Lyapunov function (21) is negative if

$$\|x\| \ge \sqrt{\frac{1}{\lambda_{\min}(Q)\lambda_{\min}(R)}}\|\xi\| \equiv \mu. \tag{22}$$

Selecting the matrices Q *and* R *such that (22) is satisfied ensures that the trajectories of (12) converge to a compact set* S_ξ *of radius* μ, *that is,* $\|x\| \le \mu$ *and hence the trajectories of (12) are UUB. Then following a similar procedure to Theorem 1 is obtained the next inequality,*

$$\begin{aligned}\dot{V} &\le -\gamma_1 V + \lambda_{\max}(R^{-1})\|\xi\|^2 \\ V(t) &\le e^{-\gamma_1(t-t_0)}V(t_0) + \frac{1}{\gamma_1\lambda_{\min}(R)}\|\xi\|^2.\end{aligned}$$

Recall that $\lambda_{\max}(R^{-1}) = \frac{1}{\lambda_{\min}(R)}$. *Finally, the states are bounded by*

$$\begin{aligned}\|x(t)\| \le \; & \sqrt{\frac{\lambda_{\max}(P)}{\lambda_{\min}(P)}}e^{-\frac{1}{2}\gamma_1(t-t_0)}\|x(t_0)\| \\ & + \sqrt{\frac{1}{\gamma_1\lambda_{\min}(P)\lambda_{\min}(R)}}\|\xi\|,\end{aligned} \tag{23}$$

and hence the states trajectories of (12) converge exponentially to the compact set S_ξ *in (22). This completes the proof.* □

4.2. Observability approach

For the observability approach [44], the closed-loop dynamics (11) can be written as,

$$\begin{aligned} \dot{x} &= A_2 x + B_2 u + \xi \\ y &= Cx \\ u &= -Ky, \end{aligned} \tag{24}$$

where $C \in \mathbb{R}^{2n\times 2n}$ is the output dynamics which for this paper is equal to a $2n \times 2n$ identity matrix. Equivalently, (24) can be rewritten as,

$$\begin{aligned} \dot{x} &= A_K x + \xi \\ y &= Cx \end{aligned} \tag{25}$$

The observability matrix of (25) is

$$\mathcal{O} = \begin{bmatrix} C^\top & (CA_K)^\top & \dots & (CA_K^{2n-1})^\top \end{bmatrix}^\top. \tag{26}$$

It is known that the system states of (25) are observable if rank$\mathcal{O} = 2n$. Equivalently, the observability of system (25) implies that the matrix,

$$W_O = \int_{t_0}^{t} e^{A_K^\top(\tau - t_0)} C^\top C e^{A_K(\tau - t_0)} d\tau, \tag{27}$$

is nonsingular for any $t > 0$ and its called observability Gramian. In contrast with the controllability matrix, the observability matrix can use either A_2 or A_K because it does not depend on the input dynamics B_2. The following theorem establishes the exponential convergence to zero of system trajectories (25) with $\xi = 0$.

Theorem 3. *Consider the robot dynamics (24) under the PD control law (8), the desired performance specified by (10) and expressed as in (25) with* $\xi = 0$*. Then there exists positive definite matrices* $Q,\ P \in \mathbb{R}^{2n\times 2n}$ *which are solution of the Lyapunov equation (15). Hence, the states of (25) converge exponentially to zero with a decay rate of* γ_2*.*

Proof 3. *The procedure is similar to the presented in Theorem 1 until the equation (17) is found. Then integrating both sides of (17) in a time interval* $[t, t+T]$*,* *where $T > 0$, gives,*

$$V(t+T) = V(t) - \int_t^{t+T} x^\top(\tau) Q x(\tau) d\tau.$$

Let $Q = C^\top C$. Then

$$\begin{aligned} V(t+T) =& V(t) \\ & - x^\top(t) \int_t^{t+T} e^{A_k^\top(\tau-t)} Q e^{A_k(\tau-t)} d\tau x(t). \end{aligned}$$

Notice that the second term of the right-hand side is equivalent to the observability Gramian (27) which is also known as uniform complete observability (UCO) and satisfies the following bounds,

$$\beta_1 I \leq W_O = \int_t^{t+T} e^{A_K^\top(\tau-t)} Q e^{A_K(\tau-t)} d\tau \leq \beta_2 I, \tag{28}$$

for some scalars $\beta_1, \beta_2 > 0$. Then multiplying the observability Gramian by $PP^{-1} = I$ gives,

$$\begin{aligned} V(t+T) &= V(t) - x^\top(t) P P^{-1} W_O x(t) \\ V(t+T) &\leq \left(1 - \frac{1}{\lambda_{\max}(P)} \beta_2\right) V(t). \end{aligned}$$

Let $\alpha = \sqrt{\frac{\lambda_{\max}(P) - \beta_2}{\lambda_{\min}(P)}}$. Then,

$$\begin{aligned} \lambda_{\min}(P) \|x(t+T)\|^2 &\leq x^\top(t+T) P x(t+T) = V(t+T) \\ &\leq (\lambda_{\max}(P) - \beta_2) \|x(t)\|^2 \\ \|x(t+T)\| &\leq \alpha \|x(t)\|. \end{aligned} \tag{29}$$

Notice that,

$$\begin{aligned} \|x(t_0+T)\| &\leq \alpha \|x(t_0)\| \\ \|x(t_0+2T)\| &\leq \alpha \|x(t_0+T)\| = \alpha^2 \|x(t_0)\| \\ &\vdots \qquad\qquad \vdots \\ \|x(t_0+kT)\| &\leq \alpha^k \|x(t_0)\|, \end{aligned}$$

where $k \in \mathbb{N}$. Define $t = t_0 + kT$, then the exponential convergence of (29) is demonstrated and can be written as,

$$\begin{aligned} \|x(t)\| &\leq \alpha^{(t-t_0)/T}\|x(t_0)\| \\ \|x(t)\| &\leq e^{-\gamma_2(t-t_0)}\|x(t_0)\| \end{aligned} \tag{30}$$

where

$$\gamma_2 = -\frac{1}{T}\ln\alpha \Leftrightarrow \gamma_2 = -\frac{1}{T}\ln\left(\sqrt{\frac{\lambda_{\max}(P)-\beta_2}{\lambda_{\min}(P)}}\right).$$

This completes the proof. □

Remark 5. *Since the eigenvalues of matrix A_K have negative real part, that is, $Re\lambda(A_K) < 0$, then the observability Gramian is a solution of the Lyapunov equation (15) with $Q = C^\top C$. Notice that the controllability Gramian (14) does not satisfy this good property because it uses the matrix A_2 which its eigenvalues could be positive or zero, that is, $Re\lambda(A_2) \geq 0$; and hence it cannot be solution of the Lyapunov equation (15).*

The following theorem establishes the exponential convergence to a bounded set of system trajectories (24) in presence of the modeling error $\xi \neq 0$.

Theorem 4. *Consider the robot dynamics (24) under the PD control law (8), the desired performance specified by (10) and expressed as in (25). Then, there exists positive definite matrices $Q, R, P \in \mathbb{R}^{2n\times 2n}$ which are solution of the Riccati equation (20) and hence, the trajectories of (25) are UUB with a practical bound μ given by (22) and converge exponentially to a bounded set S_ξ of radius μ with a decay factor γ_2 as in (30).*

Proof 4. *Consider a similar procedure to the presented in Theorem 2 such that the practical bound μ in (22) is obtained. The solution of (25) in a time interval $[t : t+T]$ is*

$$\begin{aligned} x(t+T) &= e^{A_K(t+T-t)}x(t) + \int_t^{t+T} e^{A_K(\tau-t)}\xi d\tau \\ y(t) &= Cx(t). \end{aligned} \tag{31}$$

Then,

$$y(t+T) = Ce^{A_K(t+T-t)}x(t) + C\int_t^{t+T} e^{A_K(\tau-t)}\xi d\tau.$$

Multiplying both sides of the above equality by $e^{A_K^\top(t+T-t)}C^\top$ *gives,*

$$e^{A_K^\top(t+T-t)}C^\top y(t+T) = e^{A_K^\top(t+T-t)}C^\top Ce^{A_K(t+T-t)}x + e^{A_K^\top(t+T-t)}C^\top C\int_t^{t+T} e^{A_K(\tau-t)}\xi d\tau.$$

Define $w = t+T$*. Integrating both sides of the above equality in a time interval* $[t : t+T]$ *gives,*

$$W_O x(t) = \int_t^{t+T} e^{A_K^\top(w-t)}C^\top y(w)dw - \int_t^{t+T} e^{A_K^\top(w-t)}C^\top C\int_t^{w} e^{A_K(\tau-t)}\xi d\tau dw.$$

Taking the norm in both sides and using the Cauchy Swartz inequality yields,

$$\begin{aligned}\|x(t)\| \leq & \left\| W_O^{-1}\int_t^{t+T} e^{A_K^\top(w-t)}C^\top y(w)dw\right\| \\ & + \left\| W_O^{-1}\int_t^{t+T} e^{A_K^\top(w-t)}C^\top \times \int_t^{w} Ce^{A_K(\tau-t)}\xi d\tau dw\right\| \\ \leq & \frac{\sqrt{\beta_2 T}}{\beta_1}\|y(t)\| + \frac{\beta_2\sqrt{T}}{\beta_1}\|\xi\|.\end{aligned}$$

Since $\|y(t)\| \leq \|C\|\|x(t)\|$ *with* $C = I$*, then from (22) the system states satisfy the following bound*

$$\|x(t)\| \leq \left(\frac{\sqrt{\beta_2 T}}{\beta_1}\sqrt{\frac{1}{\lambda_{\min}(Q)\lambda_{\min}(R)}} + \frac{\beta_2\sqrt{T}}{\beta_1}\right)\|\xi\| \equiv \mu_2. \tag{32}$$

So the system states of (29) converge exponentially with decay factor γ_2 *given in (30) to the bounded set* S_{ξ_2} *of radius (32). This completes the proof.* □

Remark 6. *Notice that the bound (23) of the controllability analysis depends on the initial conditions* $x(t_0)$ *which fades exponentially with a decay rate of* γ_1*. On* *the other hand, the bound (32) of the observability analysis does not depend on the initial conditions and take advantage of the observability Gramian bounds. Furthermore, the bound (32) does not need the solution P of the Riccati equation (20). Therefore, the states converges at the intersection set between the sets (23) and (32).*

Remark 7. *The error $\|e(t)\|$ remain bounded and within the compact set S_ξ or S_{ξ_2} by selecting large enough desired performance gains Λ_1 and Λ_2 respect to the linearized matrix A. The linearized matrices D, B, and B_0 play an important role for dynamic compensation and to reduce the steady state error. The matrix Q of the Lyapunov equation (15) and the matrices Q and R of the Riccati equation (20) provides an easy way to compute the exponential decay factor of the exponential solution. However, they are only theoretical parameters that do not change the performance of the closed-loop system.*

Remark 8. *The controllability and observability results hold for exogenous and bounded disturbances $d(t) \in \mathbb{R}$ that satisfy $\|d(t)\| \leq \bar{d}$ for some $\bar{d} > 0$. The modelling error ξ in (12) and (24) is modified as*

$$\xi = \begin{bmatrix} 0 \\ \bar{d} - \eta \end{bmatrix} \in \mathbb{R}^{2n}. \tag{33}$$

5. Experiments

The performance of the robust feedback linearization controller was evaluated in two different direct drive robot manipulators. The controllers are coded using Matlab/Simulink software platform under the program Wincon from Quanser Consulting. The Simulink diagrams use a sampling period of 0.1 ms and the ODE4 solver.

5.1. Control of a 1-DOF robot

The 1-DOF robot (see Figure 1) is controlled by a Copley Controls power amplifier, model 413, configured in current mode. Angular position of the motor is measured by a BEI optimal encoder. Resolution of the optical encoder is 2500 pulses per revolution and is directly coupled to the motor shaft. Angular velocity is measured by a Servo-Tek tachometer with a resolution of 7V/1000 rpm. The tachometer and encoder outputs are filtered by the following low-pass filter $G(s) = \frac{50}{s+50}$. $G(s)$ was tuned manually until the best performance was achieved.

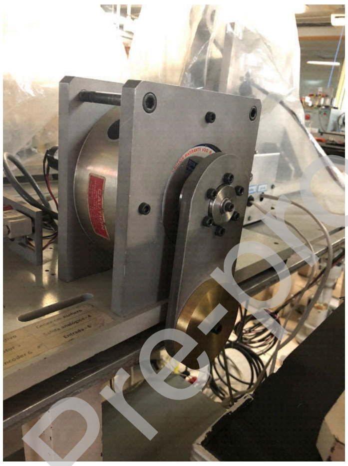

Figure 1: 1-DOF robot prototype.

Data acquisition is performed by a Sensoray model 626 PCI data acquisition target endowed with inputs for optical encoders. The data card electronics increases four times the optical encoder resolution up to 10,000 pulses per revolution. The dynamic model of the 1-DOF robot is $M\ddot{q} + R\dot{q} + G\sin(q) = u$, where $M = 0.1852$ kgm, $R = 0.019$ kgm/s and $G = 2.60$ kgm/s^2; $q, \dot{q}, \ddot{q}$ defines the angular position, velocity and acceleration, respectively. These parameters were obtained previously using a least squares method.

The linearization is performed in the operating point $O(u_l = 0, q_l = 0, \dot{q}_l = 0, \ddot{q}_l = 0)$. The linearized model is $A\ddot{q}_r + D\dot{q} + Bq = u$, where $A = 0.1852$ kgm, $D = 0.019$ kgm/s and $B = 2.60$ kgm/s^2. Notice that this robot does not have Coriolis term. For this example is easy to obtain the radius and interval of convergence of the Taylor series expansion, that is, only the gravitational term was linearized and satisfies

$$G\sin(q) = G\sum_{n=0}^{\infty}\frac{(-1)^n}{(2n+1)!}q^{2n+1} = G\left(q - \frac{q^3}{3!} + \frac{q^5}{5!} - \cdots\right)$$

Then the radius of convergence is

$$\begin{aligned}&\lim_{n\to\infty}\left|\frac{(-1)^{n+1}}{(2(n+1)+1)!}q^{2(n+1)+1}\Big/\frac{(-1)^n}{(2n+1)!}q^{2n+1}\right|\\&= \lim_{n\to\infty}\frac{(2n+1)!}{(2n+3)!}|q|^2\\&= \lim_{n\to\infty}\frac{1}{(2n+2)(2n+3)}|q|^2 = 0.\end{aligned}$$

Because this limit is zero for all real values $q \in \mathbb{R}$, then the radius of convergence of the expansion is the set of all real numbers $\mathbb{R}$.

The desired closed-loop performance is defined by the proposed values of $\Lambda_1 = 20$ and $\Lambda_2 = 100$. The Ackermann formula is used to obtain the gains of the PD controller. The performance of the linearized models (3), (4) and (6) are compared, and hence the control gains were modified in terms of each model. The models, controller and control gains that were used in the experiments are shown in Table 1.

Table 1: Linearized models and control gains

Model	**Control law**	K_p	K_d
$A\ddot{q}_r = u$	$u = K_p e + K_d\dot{q} + A\ddot{q}_d \triangleq u_1$	18.52	3.70
$A\ddot{q}_r + Bq_r = u$	$u = u_1 + Bq_d \triangleq u_2$	15.92	3.70
$A\ddot{q}_r + D\dot{q}_r + Bq_r = u$	$u = u_2 + D\dot{q}_d$	15.92	3.68

The desired reference is a chaotic duffing system of the form

$$\begin{aligned}\dot{z}_1 &= z_2\omega\pi\\ \dot{z}_2 &= [-0.25z_2 + z_1 - 1.05z_1^3 + 0.3\sin(\omega\pi t)]\omega\pi\\ q_d &= 7z_1,\ z_1(0) = z_2(0) = 0,\quad \omega = 2 \text{ rad/s}.\end{aligned} \tag{34}$$

The above reference was proposed to show the effectiveness of the robust linearization technique in presence of a trajectory that could destabilize the closed-loop system due to modeling error and the remainder of the Taylor formula. Figure 2(a) shows the tracking results using the models and controllers of Table 1.

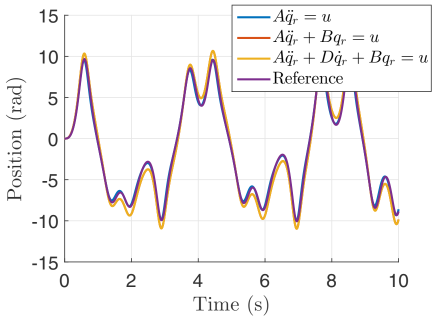

(a) Position: Tracking task

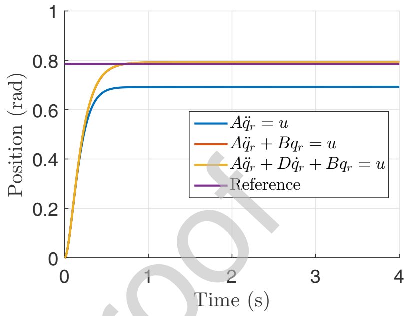

(b) Position: Set-point task

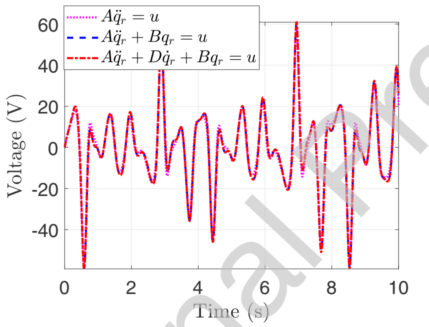

(c) Voltage: Tracking task

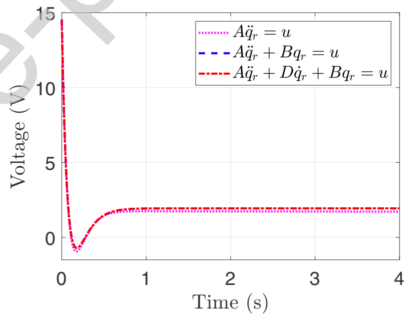

(d) Voltage: Set-point task

Figure 2: Results of the 1-DOF robot

Figure 2(a) shows some interesting results. The simplest linearization technique, $A\ddot{q}_r = u$, has better tracking results in comparison with the other linearization methods. The main reason is that PD control gains excite the modeling error dynamics and hinders accurate realization of the task. This problem is known as the "accuracy/robustness" dilemma[28]. In other words, the PD control law enhances robustness against disturbances (modeling error, remainder of Taylor series formula, exogenous perturbations, etc.). On the other hand, the PD control gains can excite the disturbances in such a way that there exists some stationary error. Since model $A\ddot{q}_r = u$ is a double integrator system, then the control gains were larger than the other models. Nevertheless, the output trajectory can present delays if the parameter A is not accurate. The second and third methods have similar results. For this simple model, the friction was small and therefore did not affect the closed-loop system trajectories. Furthermore, the desired trajectory was fast and hence the gravitational terms were compensated by the momentum of the pendulum in the swinging movement.

The double integrator system did not present good results in presence of a constant gravitational term. To show this fact, the tracking problem was modified into a set-point control. The desired trajectory was changed to a constant reference $q_d = \frac{\pi}{4}$. Figure 2(b) exhibits the obtained results. The plot shows that the double integrator system was sensitive to the gravitational terms because the PD gains cannot compensate it. The mean-squared error (MSE) $\bar{e} = \frac{1}{n}\sum_{i=1}^{n} ke^2(i)$, where k is a scaling factor and n is the number of samples; was used as metric performance. It was proposed a scaling factor $k = 100$. The MSE of both the tracking and set-point tasks is shown in Table 2.

Table 2: MSE results of the 1-DOF robot

Model	**Tracking MSE**	**Set-point MSE**
$A\ddot{q}_r = u$	7.625	0.884
$A\ddot{q}_r + Bq_r = u$	57.64	0.0035
$A\ddot{q}_r + D\dot{q}_r + Bq_r = u$	57.82	0.0036

The mean absolute value of the control voltage $\bar{u} = \frac{1}{n}\sum_{i=1}^{n} |u(i)|$ was used as performance metric of the input voltage. The results are shown in Table 3.

Table 3: Mean value of the input voltage of the 1-DOF robot

Model	**Tracking task**	**Set-point task**
$A\ddot{q}_r = u$	12.9207	1.7023
$A\ddot{q}_r + Bq_r = u$	13.33381	1.9157
$A\ddot{q}_r + D\dot{q}_r + Bq_r = u$	13.4342	1.9161

5.2. Control of a 4-DOF robot

The 4-DOF robot (see Figure 3) was controlled by Schunk PowerCube modules PR 110-161, PR 90-161 and PR 70-161 using the CAN protocol. These modules have incremental encoders RS-422 included for angular position measurements. A high-pass filter was used to estimate the angular velocity whose cutoff frequency was 300, that is, $G_1(s) = \frac{300s}{s+300}$. Also a low-pass filter with cutoff frequency of 500 was used to smooth the velocity response, that is, $G_2(s) = \frac{500}{s+500}$. Both $G_1(s)$ and $G_2(s)$ were tuned manually until the best performance was achieved.

(a) Robot prototype

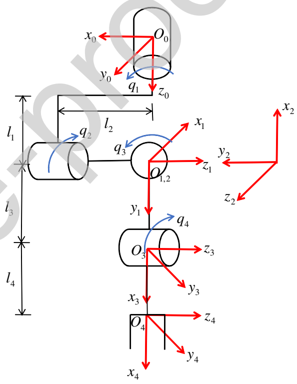

(b) Robot schematic

Figure 3: 4-DOF robot

The Denavit-Hartenberg (DH) parameters of the 4-DOF robot are given in Table 4.

The parameter estimates of the robot are exhibited in Table 5, where m_i, l_i, and I_i denote the mass, length and inertia of link i, here $*$ means that the term was not used. It is not possible to express the dynamic model in a simple and compact form due to its high non-linearity. However, the analytic expression can be easily obtained using any symbolic toolbox.

The dynamics is linearized at the operating point $O(q_l = [0, \frac{\pi}{2}+0.1, 0, 0.1]^\top)$, the other terms are set to zero. The linearized model is $A\ddot{q}_r + Bq_r + B_0 = u$,

Table 4: Denavit Hartenberg Parameters

Joint i	θ_i	$\mathbf{d}_i$	$\mathbf{a}_i$	α_i
1	q_1	l_1	0	$\frac{\pi}{2}$
2	q_2	0	0	-$\frac{\pi}{2}$
3	q_3	0	l_3	$\frac{\pi}{2}$
4	q_4	0	l_4	0

Table 5: 4-DOF parameters

Joint i	m_i **(kg)**	l_i **(m)**	I_i (kgm^2)
1	8.4	0.228	0.0364
2	4.9	*	*
3	2.7	0.22	0.0109
4	2.7	0.22	0.0109

where

$$A = \begin{bmatrix} 0.064 & 0 & -0.044 & 0 \\ 0 & 0.75 & 0 & 0.27 \\ -0.044 & 0 & 0.35 & 0 \\ 0 & 0.27 & 0 & 0.14 \end{bmatrix}, \quad B = \begin{bmatrix} 0 & -11.55 & 0 & -2.85 \\ -11.55 & 0 & 0 & 0 \\ 0 & 0 & 0 & -0.29 \\ -2.85 & 0 & -0.29 & 0 \end{bmatrix}$$

$$B_0 = \begin{bmatrix} -1.45, 0, 11.64, 0 \end{bmatrix}^\top$$

Notice that this model did not have a friction term because its parameters were unknown. Furthermore, the Coriolis term was neglected in the linearization point. For any robot, the radius of convergence of the Taylor series expansion is not straightforward to obtain analytically since each element of the matrix are functions of trigonometric functions and we cannot conclude that the radius of convergence is the $\mathbb{R}^n$ space. In this experiment, the performance of the PD control with Taylor series compensation was compared with the well-known computer torque controller

$$u = M(q)\Big(\ddot{q}_d + K_p e + K_d \dot{e}\Big) + C(q,\dot{q})\dot{q} + G(q). \tag{35}$$

The computer torque controller is a feedback linearization controller that compensates the complete robot dynamics and establishes a desired performance given by an inner controller (in most of cases is a PD control law). For this experiment, the inner controller of the computed torque is a PD control whose gains were set as the desired performance in (10), that is, $K_p = \Lambda_2$ and $K_d = \Lambda_1$.

The desired trajectory $q_d = [q_1^d, q_2^d, q_3^d, q_4^d]^\top \in \mathbb{R}^4$ was proposed to satisfy the range of movements of an human shoulder and elbow as:

$$\begin{aligned} q_1^d(t) &= 0.3\sin\left(\tfrac{\pi}{3}t\right) \\ q_2^d(t) &= \tfrac{\pi}{2} - 0.4\cos\left(\tfrac{\pi}{3}t\right) \\ q_3^d(t) &= -0.2 - 0.55\sin\left(\tfrac{\pi}{3}t\right) \\ q_4^d(t) &= 0.35 + 0.2\cos\left(\tfrac{\pi}{3}t\right). \end{aligned} \tag{36}$$

The values of the desired performance matrices were proposed as $\Lambda_1 = 10 \times \text{diag}\{12, 8, 6, 8\}$ and $\Lambda_2 = 100 \times \text{diag}\{36, 16, 9, 16\}$. The proportional and derivative matrices gains for the PD control with complete Taylor series compensation were

$$K_p = \begin{bmatrix} 229.24 & 11.55 & -39.97 & 2.85 \\ 11.55 & 1200.29 & 0 & 437.27 \\ -159.88 & 0 & 312.75 & 0.29 \\ 2.85 & 437.27 & 0.29 & 225.99 \end{bmatrix},$$

$$K_d = \begin{bmatrix} 7.64 & 0 & -2.66 & 0 \\ 0 & 60.01 & 0 & 21.86 \\ -5.33 & 0 & 20.85 & 0 \\ 0 & 21.86 & 0 & 11.3 \end{bmatrix}.$$

Figure 4 shows the tracking results. It can be observed that each feedback linearization controller exhibits good tracking results due to the proposed desired matrices Λ_1 and Λ_2. The Taylor series compensation enhances the robustness of the PD controller and reduces the steady-state error.

The PowerCube modules have large stiffness and friction unmodeled terms. These terms were favorable at the closed-loop performance of the experiment because they serve as an inner PD control law. Despite having modeling error, the proposed feedback linearization controller presents robust performance and good tracking accuracies similarly to the compute torque controller. The latter, is computationally more expensive than the PD control with Taylor series compensation due to the number of operations that it has to compute (among sums, multiplications, and standard functions). For real-time implementations the computed torque controller has the next two main components [13]

1. An inner feedback loop such as a stabilizing PD, PID, or any other controller.
2. An inverse dynamic solver to provide the torques for each joint.

In view of the above, the computer torque controller could have a relatively large time-delay due to the hardware and software limitations. The proposed feedback linearization controller overcome this issue by considering less number of operations. In fact, whilst the computational complexity of the proposed approach is $\mathcal{O}(n)$, for the computed torque controller is $O(n^2)$ [13].

The performance of each linearized model was evaluated using the MSE of the last 4 seconds of the experiment. The results are given in Table 6. From these results, it is shown that the term B_0 robustify the control law in presence of changes of the gravitational term. Furthermore, the MSE error demonstrates that a feedback linearization controller converges to a bounded zone instead of zero. This important fact verifies the proposed stability approach. Since the trajectory is slow, then the robot cannot neglect the gravitational terms as in the 1-DOF robot case and therefore the simplest linear model has large error.

The mean absolute value (MAE) of each control torque is used to compare the performance of each feedback linearization controller. The results are exhibited in Figure 5 and Table 7 where similar control torque values were shown for each feedback linearization control law with small magnitude differences. These results permit concluding that the proposed feedback linearization controller

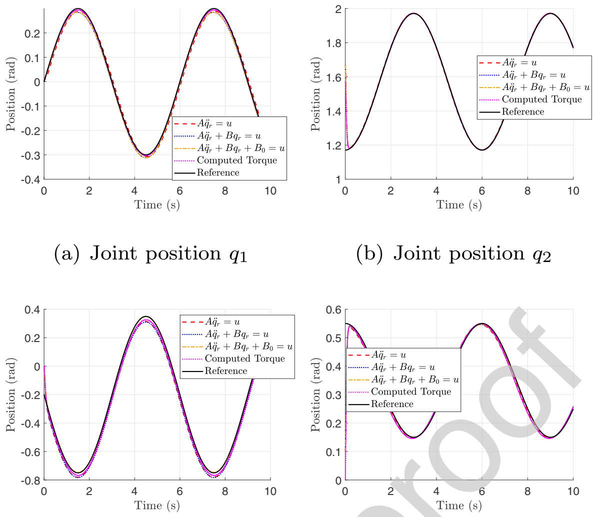

(a) Joint position q_1 (b) Joint position q_2

(c) Joint position q_3 (d) Joint position q_4

Figure 4: Joint position tracking results

Table 6: MSE results of the 4-DOF exoskeleton robot

Control	$\bar{e}_1$	$\bar{e}_2$	$\bar{e}_3$	$\bar{e}_4$
$u_1 = K_p e + K_d \dot{e} + A\ddot{q}_r + \ddot{q}_d$	0.0181	0.0819	0.1297	0.0725
$u_2 = u_1 + B(q_r - q_l)$	0.0125	0.0798	0.1522	0.0663
$u_3 = u_2 + B_0$	0.0121	0.0798	0.0163	0.0661
$u_4 = M(q)[u_1 - A\ddot{q}_r] + C(q,\dot{q})\dot{q} + G(q)$	0.0011	0.0512	0.0639	0.1067

can obtain robust performances with less computational effort and opens the opportunity to the design robust/adaptive controllers based on the linearized model.

6. Conclusions

In this paper a robust feedback linearization of robot manipulators was proposed. A linearization procedure was proposed using Taylor series expansion, which includes initial conditions and the remainder of the Taylor formula. This new linearization procedure gives a more realistic model of the robot dynamics

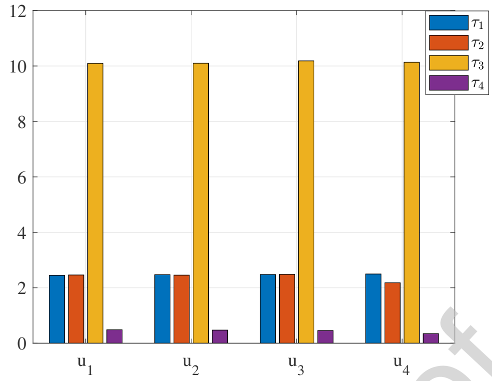

Figure 5: MAE Histogram of the control torque

Table 7: MAE results

Control	τ_1	τ_2	τ_3	τ_4
u_1	2.4485	2.4618	10.0932	0.486
u_2	2.4731	2.456	10.0998	0.4732
u_3	2.4787	2.2827	10.1847	0.4580
u_4	2.4973	2.1812	10.1357	0.3459

which not assumes that the real system will behave as its linear model.

Exponential convergence to a bounded zone was proved using Lyapunov stability theory. The stability proofs were analyzed in terms of controllability and observability theories. The main drawback of this kind of controllers is that it needs good estimates of the robot parameters which are not always available.

Experimental validation was carried out using a 1-DOF robot and an 4-DOF exoskeleton robot. Interesting results were obtained in the 1-DOF robot, since the simplest linear model had better results for tracking tasks and the worst performance for a set-point control tasks. The main reason was that the controller takes advantage of the pendulum inertia in such a way that the gravitational terms were almost neglected. Conversely, in a set-point control the simplest linear model cannot achieve good accuracy. In the exoskeleton results, the feedback linearization controller achieves robust performance in presence of modeling error.

Future work consists on developing adaptive PD control laws that adapts the desired performance in terms of the actuator limitations (torque, voltage, current) and the unmodeled system dynamics (friction, endogenous and exogenous disturbances).

Declaration of Competing Interests

The authors declare that they have no known competing financial interests or personal relationships that could have appeared to influence the work reported in this paper.

References

[1] A. Perrusquía, J. A. Flores-Campos, C. R. Torres-Sanmiguel, N. González, Task space position control of slider-crank mechanisms using simple tuning techniques without linearization methods, IEEE Access 8 (2020) 58435–58442.

[2] J. A. Flores-Campos, A. Perrusquía, L. H. Hernández-Gómez, N. González, A. Armenta-Molina, Constant speed control of slider-crank mechanisms: A joint-task space hybrid control approach, IEEE Access 9 (2021) 65676–65687.

[3] H. K. Khalil, J. W. Grizzle, Nonlinear systems, Vol. 3, Prentice hall Upper Saddle River, NJ, 2002.

[4] A. Perrusquía, W. Yu, Robust control under worst-case uncertainty for unknown nonlinear systems using modified reinforcement learning, International Journal of Robust and Nonlinear Control 30 (7) (2020) 2920–2936.

[5] R. Kelly, V. S. Davila, J. A. L. Perez, Control of robot manipulators in joint space, Springer Science & Business Media, 2006.

[6] M. W. Spong, M. Vidyasagar, Robot dynamics and control, John Wiley & Sons, 2008.

[7] A. Perrusquía, R. Garrido, W. Yu, An input error method for parameter identification of a class of euler-lagrange systems, in: 2021 18th International Conference on Electrical Engineering, Computing Science and Automatic Control (CCE), IEEE, 2021, pp. 1–6.

[8] A. Swarup, M. Gopal, Comparative study on linearized robot models, Journal of Intelligent and Robotic Systems 7 (3) (1993) 287–300.

[9] J. A. Flores-Campos, J. Perrusquía Guzmán, J. A. Beltrán-Fernández, L. H. Hernández-Gómez, Sliding mode control of a water-displacement based mechanism applied to the orientation of a parabolic-trough solar concentrator, in: Defect and Diffusion forum, Vol. 370, Trans Tech Publ, 2016, pp. 90–97.

[10] S. Tong, L. Zhang, Y. Li, Observed-based adaptive fuzzy decentralized tracking control for switched uncertain nonlinear large-scale systems with dead zones, IEEE Transactions on Systems, Man, and Cybernetics: Systems 46 (1) (2015) 37–47.

[11] A. Perrusquía, W. Yu, A. Soria, Position/force control of robot manipulators using reinforcement learning, Industrial Robot: the international journal of robotics research and application.

[12] S. Tong, S. Sui, Y. Li, Fuzzy adaptive output feedback control of mimo nonlinear systems with partial tracking errors constrained, IEEE Transactions on Fuzzy Systems 23 (4) (2014) 729–742.

[13] C. Kingsley, M. Poursina, S. Sabet, A. Dabiri, Logarithmic complexity dynamics formulation for computed torque control of articulated multibody systems, Mechanism and Machine Theory 116 (2017) 481–500.

[14] W. Yu, X. Li, R. Carmona, A novel PID tuning method for robot control, Industrial Robot: An International Journal.

[15] X. Li, W. Yu, A systematic tunning method of PID controller for robot manipulators, in: 2011 9th IEEE International Conference on Control and Automation (ICCA), IEEE, 2011, pp. 274–279.

[16] A. Perrusquía, W. Yu, A. Soria, R. Lozano, Stable admittance control without inverse kinematics, IFAC-PapersOnLine 50 (1) (2017) 15835–15840.

[17] Y. Pan, H. Yu, M. J. Er, Adaptive neural PD control with semiglobal asymptotic stabilization guarantee, IEEE Transactions on Neural Networks and Learning Systems 25 (12) (2014) 2264–2274.

[18] W. Deng, J. Yao, Asymptotic tracking control of mechanical servosystems with mismatched uncertainties, IEEE/ASME Transactions on Mechatronics.

[19] J. de Jesús Rubio, Robust feedback linearization for nonlinear processes control, ISA transactions 74 (2018) 155–164.

[20] A. Perrusquia, C. Tovar, A. Soria, J. C. Martinez, Robust controller for aircraft roll control system using data flight parameters, in: 2016 13th International Conference on Electrical Engineering, Computing Science and Automatic Control (CCE), IEEE, 2016, pp. 1–5.

[21] W. Yu, PID Control with Intelligent Compensation for Exoskeleton Robots, Academic Press, 2018.

[22] J. A. Flores Campos, A. Perrusquía, Slider position control for slider-crank mechanisms with jacobian compensator, Proceedings of the Institution of Mechanical Engineers, Part I: Journal of Systems and Control Engineering 233 (10) (2019) 1413–1421.

[23] S. Liu, P. X. Liu, X. Wang, Stability analysis and compensation of network-induced delays in communication-based power system control: A survey, ISA transactions 66 (2017) 143–153.

[24] S. M. Azimi, S. Afsharnia, A robust nonlinear stabilizer as a controller for improving transient stability in micro-grids, ISA transactions 66 (2017) 46–63.

[25] A.-T. Nguyen, T.-M. Guerra, J. Lauber, Robust feedback linearization approach for fuel-optimal oriented control of turbocharged spark-ignition engines, in: Intelligent and Efficient Transport Systems-Design, Modelling, Control and Simulation, IntechOpen, 2020.

[26] C. I. Pop, E. H. Dulf, A. Mueller, Robust feedback linearization control for reference tracking and disturbance rejection in nonlinear systems, Recent Advances in Robust Control-Novel Approaches and Design Methods (2011) 273–290.

[27] A. Perrusquía, W. Yu, Task space human-robot interaction using angular velocity jacobian, in: 2019 international symposium on medical robotics (ISMR), IEEE, 2019, pp. 1–7.

[28] A. Perrusquía, W. Yu, Human-in-the-loop control using Euler angles, Journal of Intelligent & Robotic Systems 97 (2) (2020) 271–285.

[29] W. Yu, A. Perrusquía, Simplified stable admittance control using end-effector orientations, International Journal of Social Robotics (2019) 1–13.

[30] W. Yu, J. Rosen, A novel linear PID controller for an upper limb exoskeleton, in: 49th IEEE Conference on Decision and Control (CDC), IEEE, 2010, pp. 3548–3553.

[31] A. Perrusquia, J. A. Flores-Campos, C. R. Torres-San-Miguel, A novel tuning method of PD with gravity compensation controller for robot manipulators, IEEE Access 8 (2020) 114773–114783.

[32] F. Reyes, A. Rosado, Polynomial family of PD-type controllers for robot manipulators, Control Engineering Practice 13 (4) (2005) 441–450.

[33] W. Deng, J. Yao, Y. Wang, X. Yang, J. Chen, Output feedback backstepping control of hydraulic actuators with valve dynamics compensation, Mechanical Systems and Signal Processing 158 (2021) 107769.

[34] A. Perrusquía, J. A. Flores-Campos, W. Yu, Optimal sliding mode control for cutting tasks of quick-return mechanisms, ISA transactions.

[35] M. Palanisamy, H. Modares, F. L. Lewis, M. Aurangzeb, Continuous-time q-learning for infinite-horizon discounted cost linear quadratic regulator problems, IEEE transactions on cybernetics 45 (2) (2014) 165–176.

[36] D. Cobb, Controllability, observability, and duality in singular systems, IEEE transactions on Automatic Control 29 (12) (1984) 1076–1082.

[37] Z. Wang, H. Zhang, W. Yu, Robust exponential stability analysis of neural networks with multiple time delays, Neurocomputing 70 (13-15) (2007) 2534–2543.

[38] T. Berger, T. Reis, Controllability of linear differential-algebraic systemsa survey, in: Surveys in differential-algebraic equations I, Springer, 2013, pp. 1–61.

[39] C.-T. Chen, Linear system theory and design, Oxford University Press, 1999.

[40] J. O. Escobedo, V. Nosov, J. A. Meda, Minimum number of controls for full controllability of linear time-invariant systems, IEEE Latin America Transactions 14 (11) (2016) 4448–4453.

[41] V. K. Mishra, N. K. Tomar, Controllability analysis of linear time-invariant descriptor systems, IFAC-PapersOnLine 49 (1) (2016) 532–536.

[42] F. Lewis, S. Jagannathan, A. Yesildirak, Neural network control of robot manipulators and non-linear systems, CRC press, 1999.

[43] A. Perrusquía, W. Yu, Neural $\mathcal{H}_2$ control using continuous-time reinforcement learning, IEEE Transactions on Cybernetics.

[44] N. P. Salau, J. O. Trierweiler, A. R. Secchi, Observability analysis and model formulation for nonlinear state estimation, Applied Mathematical Modelling 38 (23) (2014) 5407–5420.

2022-01-07

Robust state/output feedback linearization of direct drive robot manipulators: a controllability and observability analysis

Perrusquía, Adolfo

Elsevier

Perrusquía A. (2022) Robust state/output feedback linearization of direct drive robot manipulators: a controllability and observability analysis. European Journal of Control, Volume 64, March 2022, Article number 100612

https://doi.org/10.1016/j.ejcon.2021.12.007